



ELSEVIER

Contents lists available at ScienceDirect

BBA - Biomembranes

journal homepage: [www.elsevier.com/locate/bbamem](http://www.elsevier.com/locate/bbamem)

## Diverse residues of intracellular loop 5 of the Na<sup>+</sup>/H<sup>+</sup> exchanger modulate proton sensing, expression, activity and targeting

Ka Yee Wong<sup>a</sup>, Ryan McKay<sup>b</sup>, Yongsheng Liu<sup>a</sup>, Kaitlyn Towle<sup>b</sup>, Yesmine Elloumi<sup>a</sup>, Xiuju Li<sup>a</sup>, Sicheng Quan<sup>a</sup>, Debajyoti Dutta<sup>a</sup>, Brian D. Sykes<sup>a</sup>, Larry Fliegel<sup>a,\*</sup>

<sup>a</sup> Dept of Biochemistry, University of Alberta, Canada

<sup>b</sup> Dept of Chemistry, University of Alberta, Canada

### ARTICLE INFO

#### Keywords:

Alanine scanning mutagenesis  
Intracellular loop  
Intracellular pH  
Membrane protein  
Na<sup>+</sup>/H<sup>+</sup> exchanger  
NMR

### ABSTRACT

The mammalian Na<sup>+</sup>/H<sup>+</sup> exchanger isoform 1 (NHE1) is an integral membrane protein that regulates intracellular pH (pH<sub>i</sub>) by removing a single intracellular proton in exchange for one extracellular sodium ion. It is involved in cardiac hypertrophy and ischemia reperfusion damage to the heart and elevation of its activity is a trigger for breast cancer metastasis. NHE1 has an extensive 500 amino acid N-terminal membrane domain that mediates transport and consists of 12 transmembrane segments connected by intracellular and extracellular loops. Intracellular loops are hypothesized to modulate the sensitivity to pH<sub>i</sub>. In this study, we characterized the structure and function of intracellular loop 5 (IL5), specifically amino acids 431–443. Mutation of eleven residues to alanine caused partial or nearly complete inhibition of transport; notably, mutation of residues L432, T433, I436, N437, R440 and K443 demonstrated these residues had critical roles in NHE1 function independent of effects on targeting or expression. The nuclear magnetic resonance (NMR) solution spectra of the IL5 peptide in a membrane mimetic sodium dodecyl sulfate solution revealed that IL5 has a stable three-dimensional structure with substantial alpha helical character. NMR chemical shifts indicated that K438 was in close proximity with W434. Overall, our results show that IL5 is a critical, intracellular loop with a propensity to form an alpha helix, and many residues of this intracellular loop are critical to proton sensing and ion transport.

### 1. Introduction

The mammalian Na<sup>+</sup>/H<sup>+</sup> exchanger, type I isoform (NHE1), is a key pH regulatory protein. NHE1 is ubiquitously expressed across species as a plasma membrane protein and catalyzes the removal of a single intracellular proton in exchange for a single extracellular sodium ion [1]. Beyond the regulation of intracellular pH (pH<sub>i</sub>), NHE1 is indirectly involved in many physiological and pathological roles. Physiologically it facilitates: inward sodium flux in response to osmotic shrinkage, the promotion of cell growth, differentiation [2], and enhances cell motility [3]. In pathology, NHE1 is also implicated in breast cancer cell invasiveness; specifically NHE1 activity enhances invasion by breast cancer cells by raising pH<sub>i</sub> and acidifying extracellular microenvironment of tumour cells [4–7]. Extracellular acidification may be necessary for protease activation, which facilitates the digestion and remodeling of the extracellular matrix that is critical in metastasis [5]. NHE1 is also involved in the myocardium in another pathological role. It promotes heart hypertrophy and amplifies the damage that occurs during myocardial ischemia and reperfusion. In preclinical trials, it has

been proven that inhibition of NHE1 protects the myocardium from ischemia-reperfusion damage [8–11]. However, clinical trials did not show the same result, possibly due to a lack of specificity of the inhibitors [12]. A deeper understanding of the structure and the function of NHE1 can facilitate the development of more specific inhibitors for clinical use.

Putatively, the mammalian NHE1 protein consists of 12 transmembrane (TM) segments; an N-terminal region of approximately 500 amino acids and a long cytosolic tail. These TM segments are connected by a series of intracellular loops (IL) and extracellular loops (EL). These loops are significant because their presence and composition influence the arrangements and packing of TM segments [13]. In addition, they can modulate protein function [14]. Previous studies have mostly examined ELs such as EL5, which turned out to be involved in drug sensitivity and cation binding [15, 16]. Additionally, EL2 links TM segments I and II and mutations of residues of EL2 have been shown to affect both the drug sensitivity and the activity of NHE1 [17, 18]. There were two models of NHE1 structure. One is based on cysteine accessibility studies [19] and the second based on computational comparison

\* Corresponding author at: Department of Biochemistry, University Alberta, Edmonton, AB T6G 2H7, Canada.

E-mail addresses: [ryan.mckay@ualberta.ca](mailto:ryan.mckay@ualberta.ca) (R. McKay), [lfiiegel@ualberta.ca](mailto:lfiiegel@ualberta.ca) (L. Fliegel).

<https://doi.org/10.1016/j.bbamem.2018.07.014>

Received 6 June 2018; Received in revised form 26 July 2018; Accepted 27 July 2018

Available online 31 July 2018

0005-2736/ © 2018 Elsevier B.V. All rights reserved.

with the deduced structure of the *Escherichia coli* Na<sup>+</sup>/H<sup>+</sup> exchanger NhaA [20]. However, recently we demonstrated that the model based on cysteine accessibility is correct with regard to C-terminal part of the membrane domain [21]. Both models place amino acids of IL5 in an intracellular location.

A previous study [22] has demonstrated that some individual changes to charged amino acids in intracellular loops could affect NHE1 function. With the knowledge that these regions are important in NHE1 function, we used a combination of two approaches to study the region. NMR was used to characterize the structural properties of a synthetic peptide of IL5, and site-specific mutagenesis characterized amino acid residues of IL5 (amino acids 431–443). The results are the first complete analysis of this region of the protein and confirm that many residues of this region are critical in NHE1 function.

## 2. Materials and methods

### 2.1. Materials

The IL5 sequence (acetyl-<sup>431</sup>GLTWFINKFRIVK<sup>443</sup>-amine) used in this study was commercially obtained from Biomatik. Norell 502 model NMR tubes were obtained from Norell Inc. (NC, USA). Deuterated (D<sub>25</sub> 98%) sodium dodecyl sulfate (SDS) was purchased from Sigma-Aldrich (Darmstadt, Germany). PWO DNA polymerase was from Roche Molecular Biochemicals, (Mannheim, Germany). Sulfo-NHS-SS-biotin was from Pierce, Rockford, IL, USA. LIPOFECTAMINE™ 2000 Reagent was from Invitrogen Life Technologies (Carlsbad, CA, USA). Anti-HA-antibody was from Santa Cruz Biotechnology (Santa Cruz, CA). BCECF-AM was from Molecular Probes, Inc. (Eugene, OR). All other chemicals were of analytical grade and were purchased from Fisher Scientific (Ottawa, ON), Sigma or BDH (Toronto, ON).

### 2.2. NMR spectroscopy in DMSO

For the initial sample, 2.8 mg of IL5 peptide was dissolved in 600 μL deuterated DMSO to a final concentration of ~2.8 mM. NMR spectra were acquired on an Agilent VNMRs 700 MHz spectrometer, equipped with an HCN cold-probe and Z-axis pulsed field gradients. For side chain chemical shift assignments, the following experiments were performed: 1D-<sup>1</sup>H, 2D-<sup>1</sup>H,<sup>1</sup>H-TOCSY, and a 2D-<sup>1</sup>H,<sup>1</sup>H-NOESY. NMR restraints used for 3D structure generation were automatically selected by CYANA 2.1 [23] based the 2D <sup>1</sup>H,<sup>1</sup>H-TOCSY manual assignments [24] and ‘clean’ 2D <sup>1</sup>H,<sup>1</sup>H-NOESY peak list. The term ‘clean’ refers to filtering the raw list of NOE peaks for non-interatomic (diagonal) peaks and any artifacts (e.g. dispersive peak shape, or existence of repetitive frequency ridges, etc.). Only the highest confidence peaks were submitted to Cyana for automated NOE assignment (see Table 1). Data were processed with NMRPipe [25] and analyzed with NMRView [26].

### 2.3. NMR spectroscopy in SDS

The IL5 peptide (pH ~6, uncorrected for deuterium isotope effect) was dissolved in 585 μL of H<sub>2</sub>O with 58.5 μL of D<sub>2</sub>O (90:10 ratio) with a final SDS concentration of 440 mM. The 10% D<sub>2</sub>O is used as an internal NMR lock solvent. Final peptide concentration was ~5 mM. SDS was added to at least 80-fold higher concentration than the peptide to ensure proper micelle formation and to limit the number of peptide molecules per micelle. We added an extra 10% SDS and this came to a final concentration of 440 mM.

NMR spectra of the SDS/micelle peptide sample were acquired on a Varian Inova 600 MHz spectrometer, equipped with an HCN triple resonance probe with Z-axis pulsed field gradient. For side chain chemical shift assignments 2D <sup>1</sup>H,<sup>1</sup>H-TOCSY and 2D <sup>1</sup>H,<sup>1</sup>H-NOESY were used to confirm assignments in ambiguous regions. NMR restraints used for 3D structure generation were automatically obtained from CYANA 2.1 using the 2D <sup>1</sup>H,<sup>1</sup>H-TOCSY assignments (as above) and 2D <sup>1</sup>H,<sup>1</sup>H-

**Table 1**  
CYANA 2.1 statistics for IL5 peptide structural calculations.

Stage	1	2	3	4	5	6	7	Refine
Peaks:								
selected	547	547	547	547	547	547	547	
assigned	422	430	423	424	414	413	414	
unassigned	125	117	124	123	133	134	133	
with diagonal assignment	0	0	0	0	0	0	0	
Cross peaks:								
with off-diagonal assignment	422	430	423	424	414	413	414	
with unique assignment	147	235	267	284	293	305	301	
with short-range assignment $ i-j  \leq 1$	348	339	332	328	325	320	318	
with medium-range assignment $1 <  i-j  < 5$	74	85	86	90	83	87	90	
with long-range assignment $ i-j  \geq 5$	0	6	5	6	6	6	6	
Upper distance limits:								
Total	241	223	227	217	211	208	255	255
short-range, $ i-j  \leq 1$	182	154	158	144	145	140	165	165
medium-range, $1 <  i-j  < 5$	59	69	66	69	63	65	85	85
long-range, $ i-j  \geq 5$	0	0	3	4	3	3	5	5
Average assignments/constraint	3.47	2.3	1.72	1.61	1.51	1.47	1	1
Average target function value	3.94	2.69	6.25	1.14	0.32	0.19	0.39	0.3
RMSD (Residues 1–13):								
Average backbone RMSD to mean	1.06	0.56	0.3	0.41	0.39	0.5	0.28	0.24
Average heavy atom RMSD to mean	1.69	0.87	0.54	0.65	0.61	0.68	0.46	0.37

NOESY ‘cleaned’ peak list. Only the highest confidence peaks were submitted to Cyana for automated NOE assignment (see Table 1). Data were processed with NMRPipe [25] and analyzed with NMRView [27].

### 2.4. Site-directed mutagenesis

Mutations were made to an expression plasmid pYN4+ containing a tagged human NHE1 isoform of the Na<sup>+</sup>/H<sup>+</sup> exchanger. The plasmid pYN4+ contains the cDNA of the entire coding region of human NHE1. It has a C-terminal hemagglutinin (HA) tag that we have previously shown does not affect activity [28]. PWO DNA polymerase (Roche Molecular Biochemicals, Mannheim, Germany) was used for amplification and site-directed mutagenesis was performed using the Stratagene (La Jolla, CA, USA) QuikChange™ site directed mutagenesis kit following the recommendations of the manufacturer. Mutations were used to change the indicated amino acids to alanine and were designed to create or remove a restriction enzyme site for use in screening transformants (Table 2). An additional series of mutations was done to change R440 and K438 to D. The fidelity of DNA amplification was confirmed by DNA sequencing.

### 2.5. Cell culture and stable transfection

To examine effects of mutations on NHE1 activity, we expressed the NHE1 protein in AP-1 cells (a Chinese hamster ovary cell line that are devoid of their own NHE1 protein). AP-1 cells were grown in a humidified atmosphere of 5% CO<sub>2</sub> in growth medium consisting of α-MEM supplemented with 10% (v/v) bovine growth serum, 25 mM HEPES, penicillin (100 U/mL) and streptomycin (100 μg/mL), pH 7.4 at 37 °C. The transfection and selection of stable cell lines was carried out as described previously and transfection was done with LIPOFECTAMINE™ 2000 Reagent [28]. Briefly, 1.0 × 10<sup>6</sup> cells were placed in 60 mm Petri dish, in 4 mL of growth media. Cells were grown until 90%

**Table 2**

Oligonucleotide primers for site-directed mutagenesis. Bold indicates restriction site introduced. Lower case indicates changed base pair.

Mutation	Sequence	Restriction site
G431A	5'CGCGTGTGGGGG <b>GCTaGc</b> CCTGACCTGGTTCATCAAC3'	<i>NheI</i>
L432A	5'CTGGGGGTGCTGGG <b>Gcgc</b> ACCTGGTTCATCAAC3'	<i>NarI</i>
T433A	GCTGGGGGTGCTGGGG <b>GCTag</b> CCTGGTTCATCAACAAG3'	<i>NheI</i>
W434A	5'CGTGTGGGGGTGCTa <b>GGCCTG</b> ACCgcGTTTCATCAACAAGTCC3'	<i>StuI</i>
F435A	5'GTGCTGGCCCTGACCTGGgc <b>CATtAAt</b> AAGTTCGGTATCGTGAAGCTG3'	<i>AseI</i>
I436A	5'GGCCTGACCTGGT <b>Tc</b> ggaACAAGTTCGGTATC3'	<i>NruI</i>
N437A	5'CTGACCTGGTTCAT <b>Cgc</b> gAAGTTCGGTATCGTG3'	<i>NruI</i>
K438A	5'GACCTGGTTCATCA <b>Cgc</b> gTTCGGTATCGTGAAGC3'	<i>MruI</i>
F439A	5'GGTTCATCAACAAGgc <b>CCGTATCGTGAAGCT</b> TACCCCAAGGACCAG3'	<i>HindIII</i>
R440A	5'GTTTCATCAACAAGT <b>Tc</b> gga <b>ATCGTGAAGCTG</b> ACC3'	<i>PvuI</i>
I441A	5'CTGGGCCTGACCTGGT <b>CATtAAt</b> AAGTTCGGTgcCGTGAAGCTGACCCCAAG3'	<i>AseI</i>
V442A	5'CAACAAGTTCGGTAT <b>Cgc</b> g <b>GAAGCT</b> TACCCCAAGGACCAG3'	<i>HindIII</i>
K443A	5'CAAGTTCGGTATCG <b>Tage</b> GCTGACCCCAAGGACCAG3'	<i>AfeI</i>
K438D	5'GTGCTGGCCCTGACCTGG <b>TTCATtAAt</b> gacTTCGGTATCGTGAAGCTGAC3'	<i>AseI</i>
R440D	5'GGTTCATCAACAAGT <b>Tc</b> gga <b>TATCGTGAAGCTG</b> ACCCCAAG3'	<i>EcoRV</i>

confluent and were transfected with 4  $\mu$ g of wild type or 4  $\mu$ g mutant plasmids. Post-transfection, trypsin was added to cells and diluted 10 or 100 times with  $\alpha$ -MEM medium. This was plated in 100 mm dishes in  $\alpha$ -MEM media containing 800  $\mu$ g/mL with geneticin (G418) that was used to maintain selection pressure without acute acid load selection. After the initial selection, single clones of transfected cells were collected, stable cell lines were maintained in 400  $\mu$ g/mL G418 and were regularly re-establish from frozen stocks at passage numbers between 5 and 15. Results shown are from at least two independently obtained clones for each mutant cell line. After screening > 100 colonies, for unknown reasons, it was still not possible to isolate a stable cell line of mutant W434A. Therefore, we examined it via transient transfections with LIPOFECTAMINE™ 2000 Reagent. Results with the W434A mutant containing cells were compared to transient transfections with wild type NHE1 protein.

## 2.6. SDS-PAGE and immunoblotting

Western blot analysis was used to confirm NHE1 expression [29]. For each western blot, 100  $\mu$ g of total cell lysate was resolved on 10% SDS and successfully transferred to nitrocellulose. Immunoblot analysis with anti-HA antibody tag compared NHE1 expression levels in samples of cell lysates of transfected AP-1 cells [29]. The Amersham enhanced chemiluminescence Western Blotting and detection system was used to detect immunoreactive proteins. Densitometry analysis of X-ray film was performed using NIH Image software (National Institutes of Health, Bethesda, MD, USA).

## 2.7. Cell surface expression

Cell surface expression was measured as described earlier [28, 29] to ensure that all mutant proteins were properly targeted to the cell surface. Briefly described, cells were labeled with Sulpho-NHS-SS-Biotin and immobilized streptavidin resin was used to remove surface labeled protein. The total and unbound proteins in equal amounts were analyzed by 10% SDS-PAGE followed by western blotting against the HA tag. The relative amounts of NHE1 on the cell surface were calculated by comparing both the 110 kDa and the 95 kDa forms of NHE1 in the total and unbound fractions respectively. Direct measurement of extracellular NHE1 protein was not possible because it was not feasible to efficiently elute biotin labeled proteins bound to immobilized streptavidin resin.

## 2.8. $\text{Na}^+/\text{H}^+$ exchange activity

NHE1 activity was measured using a PTI Deltascan spectrofluorometer as described previously [30]. Stably transfected cells were

placed on glass coverslips ( $2 \times 10^5$  cells per coverslip) and grown until they reached 80–90% confluence. The coverslip was then transferred to a cuvette holder with constant stirring by a magnetic stir bar at 37 °C. The cells were loaded with 0.15  $\mu$ g/mL 2',7-bis (2-carboxyethyl)-5-carboxyfluorescein-AM (BCECF-AM) and incubated in "Normal buffer" which contains 135 mM NaCl, 5 mM KCl, 1 mM  $\text{MgCl}_2$ , 1.8 mM  $\text{CaCl}_2$ , 5.5 mM glucose, and 10 mM HEPES, pH 7.3 at 37 °C for 20 min. Normal buffer is ostensibly bicarbonate free. Intracellular acidosis was induced by  $\text{NH}_3/\text{NH}_4^+$  pre-pulse (i.e. 3 min in "Normal buffer" containing 50 mM  $\text{NH}_4\text{Cl}$ , pH 7.3), followed by withdrawal for 30 s in " $\text{Na}^+$  free buffer": (135 mM *N*-methyl-D-glucamine, 5 mM KCl, 1 mM  $\text{MgCl}_2$ , 1.8 mM  $\text{CaCl}_2$ , 5.5 mM glucose, and 10 mM HEPES, pH 7.4). Intracellular pH ( $\text{pH}_i$ ) recovery was in "Normal buffer" allowing the cells to recover for at least 3 min in the presence of 135 mM NaCl. For every experiment, a three-point pH calibration curve was made using the  $\text{K}^+$ /nigericin method with  $\text{Na}^+$  free calibration buffers (135 mM *N*-methyl-D-glucamine, 5 mM KCl, 1 mM  $\text{MgCl}_2$ , 1.8 mM  $\text{CaCl}_2$ , 5.5 mM glucose, and 10 mM HEPES, pH 6, 7, 8) and 10  $\mu$ M nigericin [16]. The buffering capacity of the cells was determined as described earlier [16, 31]. The slope of the first 20 s of the recovery period in 135 mM NaCl represents the proton flux via NHE1 protein. Proton flux of the  $\text{Na}^+/\text{H}^+$  exchanger activity was determined as previously detailed [16, 31]. Experiments comparing the activities of wild type and NHE1 mutants were done in pairs and cells were grown to the same degree of confluence and with the same media.

## 2.9. Structure calculations

A family of solution structures for the IL5 peptide were calculated using CYANA 2.1 [23], using the NOE (nuclear Overhauser effect) restraints obtained from a 2D-NOESY experiment [32, 33]. Peaks were manually picked and chemical shift assigned from 1D- $^1\text{H}$ , 2D- $^1\text{H}$ ,  $^1\text{H}$ -TOCSY and NOESY based experiments. NOEs were selected and calibrated within CYANA according to cross-peak intensities. After seven rounds of calculation (10,000 steps per round) a total of 547 NOE restraints were unambiguously assigned, and from these 414 NOEs were used during the final round of structural calculation (Table 1). One hundred structures were generated per round, and the 20 lowest energy conformations (without NOE violations > 0.3 Å or residues in the disallowed region of the Ramachandran plot; see Supplementary Materials) were chosen to represent the average. Coordinates for IL5 peptide have been deposited in the Protein Data Bank ID D\_1000228241 and PDBID: 6BJF. Figures were generated using PyMOL Molecular Graphics System, Version 1.8 Schrödinger, LLC [34] including electrostatic surface calculations computed with the optional Adaptive Poisson-Boltzmann Solver tools [35].

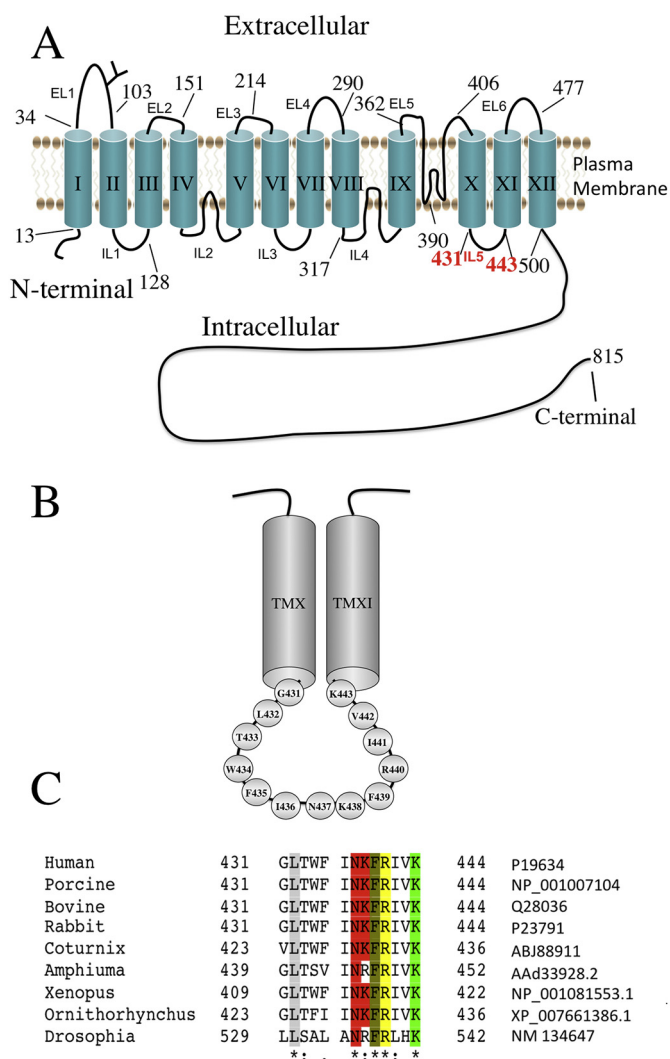


**Fig. 1.** Position and sequence of intracellular loop 5 (IL5) of the NHE1 isoform of the  $\text{Na}^+/\text{H}^+$  exchanger. **A**, Topological model of the transmembrane domain of the NHE1 based on [21]. The position of IL5 is indicated. **B**, Detailed model of IL5 illustrating individual amino acids. **C**, Alignment of amino acid sequence of IL5 and surrounding region of various NHE1 proteins. The alignment was made manually. The shaded region (\*) is where the amino acids are conserved amongst those species. The last column indicates Genbank accession numbers in the program BLAST.

### 3. Results

#### 3.1. Characterization of IL5 protein

A model of IL5 with amino acids G431-K443 is shown in Fig. 1A,B. IL5 connects TM 10 and TM 11 of the exchanger. It contains several acidic residues and a mixture of hydrophilic and hydrophobic residues and is the last intracellular loop present. It is well conserved across most species, particularly in the more distal half over the last 6 amino acids (Fig. 1C).

To characterize the structure of the IL5 we used a strategy we have earlier employed for extra-membrane domains, examination of a synthetic peptide of the region by NMR spectroscopy [17, 36]. Earlier studies have demonstrated that the structure of extra-membrane regions of membrane proteins determined by NMR corresponds well to the structures of the corresponding regions in the crystal structure of intact full length proteins [37]. Initially we attempted to use DMSO as a mimetic of the hydrophobic environment of the membrane. Preliminary  $1\text{D}^1\text{H}$  NMR spectra in deuterated DMSO were acquired at 18, 20, 27,

35 and 45 °C (Fig. 2A). As shown in Fig. 2A, temperatures above 18 °C showed peak clustering especially in the region from  $\sim 7.0$  to 7.4 ppm. Spectra acquired at 18 °C showed the best resolution of peaks in the downfield amide region and therefore subsequent 2D spectra were obtained at this temperature. Attempts at automated structure generation with a preliminary  $2\text{D}^1\text{H},^1\text{H}$ -NOESY spectrum, indicated that the peptide was unstructured in DMSO.

To explore if the IL5 loop had definitive structure in a different solvent, we obtained  $1\text{D}^1\text{H}$  NMR spectra at 40, 35, 30 and 27 °C in 440 mM SDS buffer solution (10%  $\text{D}_2\text{O}/90\%$   $\text{H}_2\text{O}$ ). As shown in Fig. 2B, the spectra were quite different when compared to the spectra taken in DMSO. All of the amide NH resonances could be resolved in the spectra taken in the presence of SDS micelles at temperatures above 27 °C and were at a uniform intensity, although the line widths were slightly larger. A comparison of the NMR spectra of the IL5 peptide in DMSO and SDS solutions at their optimal temperatures is shown in Fig. 2S. We therefore selected 27 °C in SDS for the acquisition of 2D spectra destined for final analysis. The spectra of the IL5 peptide in SDS buffer solution was fully assigned (see previous section), and NOE cross-peaks carefully picked based on absorptive shape. (The presence of artifacts in those regions (e.g. T1 noise ridges, dispersive characteristics and/or multiple diagonals) disqualified peak selection.) Structures generated using CYANA 2.1 (see Table 1) indicated that IL5 peptide is alpha helical, and when torsion angles were evaluated and presented in the Ramachandran plot (see Fig. 1S), we see that no residues were in the disallowed regions.

The chemical shift assignment from the  $2\text{D}^1\text{H},^1\text{H}$ -TOCSY (cross peaks resulting from through bond spin-spin coupling between protons) and  $2\text{D}^1\text{H},^1\text{H}$ -NOESY (cross peaks resulting from NMR close inter-nuclear distances between protons) (Fig. 3S) did contain some ambiguities due to several peak overlaps, but assignments were completed and a preliminary structure generated. The combination of the TOCSY and NOESY spectra allowed confident assignment and subsequent structure generation.

The preliminary CYANA 2.1 structures for the peptide in DMSO all gave indications of an essentially random coil. The sample in SDS, did however, show a strong indication of defined structure from the concentration and diversity of NOE cross-peaks and the improved chemical shift separation of resonances in the  $1\text{D}^1\text{H}$ . Assignments were completed and NOE cross-peaks automatically assigned by CYANA. The representative structures of the peptide in SDS micelles are shown in Fig. 3A–D and electrostatic surfaces displayed in Fig. 3E,F. We can see from the figures that the arginine and lysine residues result in a very negatively charged peptide, with residue R440 (red) at the center of a charged pocket. Fig. 3G–I show that the side chain of K438 is positioned close to the W434 aromatic ring.

We subjected IL5 to both site-specific mutagenesis and alanine scanning mutagenesis. For alanine scanning mutagenesis all residues of IL5 were changed to non-polar and hydrophobic alanine in the WT NHE1 protein. Alanine is a small hydrophobic helix forming amino acid that is small and non-intrusive [38]. In addition to alanine scanning mutagenesis, the two polar and positively charged residues R440 and K438 were mutated into polar and negatively charged aspartate (D) residues, R440D and K438D.

We first examined the expression levels, surface targeting and activity of mutant NHE1 proteins expressed in AP-1 cells. Fig. 4 shows these results. Expression levels were determined by western blotting with antibody against the HA tag on the  $\text{Na}^+/\text{H}^+$  exchanger protein. Fig. 4A–C indicates that all of the mutant proteins were expressed. We were able to obtain stable cell lines for all the mutant proteins except for W434A. For W434A, despite screening over 100 colonies, we were unable to obtain a stable cell line for unknown reasons. We therefore characterized this protein using transient transfections. As published earlier [28], NHE1 was expressed as both a fully glycosylated (110 kDa) and a partial or de-glycosylated (95 kDa) protein, and these two immunoreactive bands (Fig. 4A, B) were present in all stable cell lines and

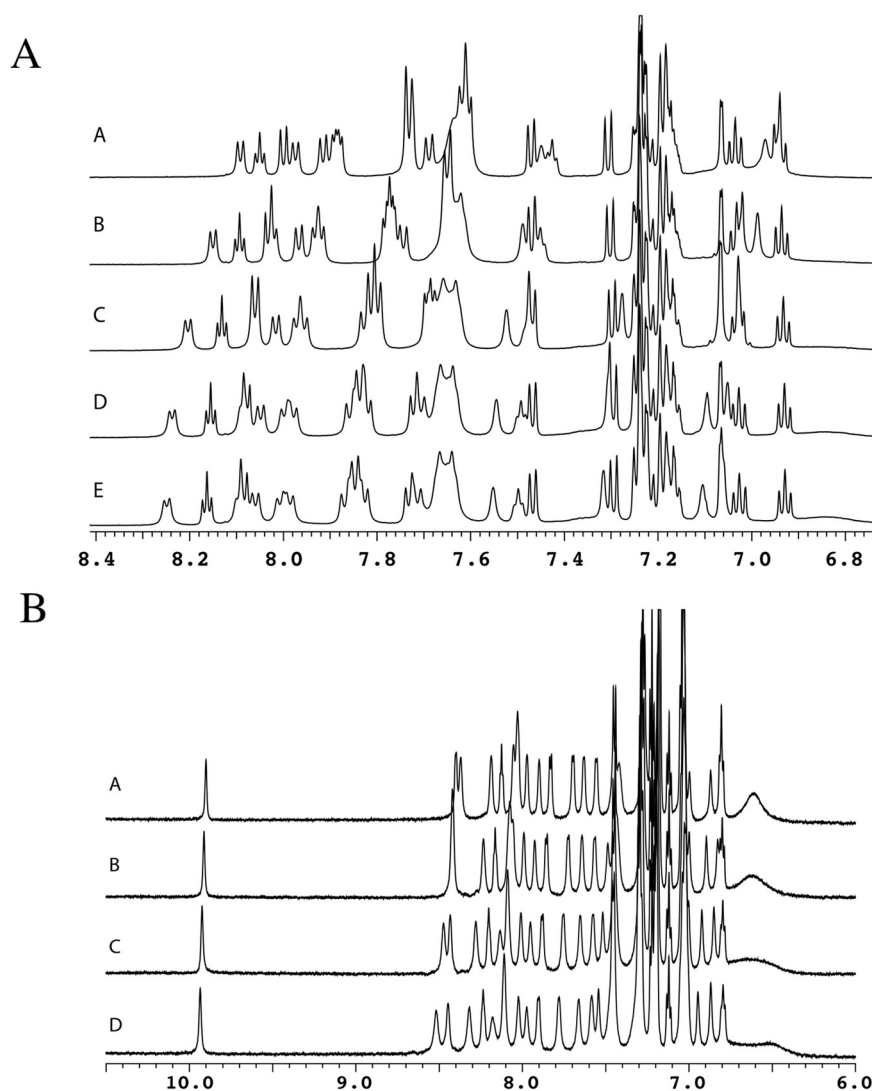


**Fig. 2.**  $^1\text{H}$  1D NMR monitored temperature titrations of IL5 peptide. A, Temperature titration of 2.8 mM IL5 peptide in DMSO. Spectra were acquired at 18, 20, 27, 35 and 45 °C (E to A) The aromatic and amide NH regions of the  $^1\text{H}$  1D NMR spectra are shown. B, Temperature titration of IL5 peptide in 440 mM SDS at 27 °C, 30 °C, 35 °C and 40 °C (D to A) 1H-1D spectra. The indole NH, amide NH, and aromatic regions of the  $^1\text{H}$  1D NMR spectra are shown.

transiently transfected cells. Expression levels of several of the mutant proteins were reduced (Fig. 4A,B). Most notably, the expression level of F435A protein was about 10% of the level of WT protein. The mutants L432A, T433A, I436A, F439A, K443A, K438D also had reduced expression that was between 30% and 50% of WT. The mutants N437A and V442A had reduced expression that was about half of the WT protein. The remaining K438A, R440A, and R440D had some slight decrease in expression compared to the WT protein. However, both G431A and I441A had expression levels that were greater than the WT protein. For the transiently transfected W434A protein, there was only a slight decrease in expression compared to WT transiently transfected protein (Fig. 4C). The expression pattern of the transiently transfected protein was slightly different than the stably transfected protein, with the amount of un- or deglycosylated protein increased relative to the mature protein. This was true for both WT and mutant W434A protein and could be due to a higher level of overexpression of the protein from the transient transfection.

We examined the surfacing targeting of the mutant proteins. Cell surface biotinylation experiments were done as described earlier [39]. Most of the mutant proteins of the stable cell lines and transiently transfected cells (W434A) were well targeted to the cell surface (70–90%, Fig. 4D, E). However, the K438A protein averaged only about

50% targeting to the cell surface and L432A, T433A, and N437A proteins were also slightly lower than wild type. Mutant W434A cell surface targeting was similar to, though slightly elevated, in comparison to the wild type protein.

We next examined the activity of the  $\text{Na}^+/\text{H}^+$  exchanger in wild type and IL5 mutants with and without corrections for levels of expression and surface targeting. Fig. 5A shows an example of  $\text{Na}^+/\text{H}^+$  exchanger activity. Cells are initially allowed to equilibrate after BCECF loading. Then  $\text{NH}_4\text{Cl}$  is added which causes an initial alkalization. Three minutes later, media was changed to ammonium chloride free and sodium free medium, which causes acidosis. Reintroduction of NaCl allows recovery from the activity of the  $\text{Na}^+/\text{H}^+$  exchanger. An example of the recovery phase of an inactive mutant (R440A) and untransfected AP-1 cells is shown for comparative purposes. Fig. 5B, C show  $\text{Na}^+/\text{H}^+$  exchanger activity of both uncorrected and corrected IL5 mutants. AP-1 cells had < 5% of the WT protein, and only I441A had activity comparable to WT. The mutant proteins G431A, K438A, V442A, K438D and R440D had uncorrected activity between 40 and 70% of WT protein. The mutant proteins N437A, F439A and K443 had uncorrected activity 25 to 40% of WT protein and the mutant proteins L432A, T433A, F435A, I436A and R440A had uncorrected activity only slightly greater than background levels, approximately 10–20% that of

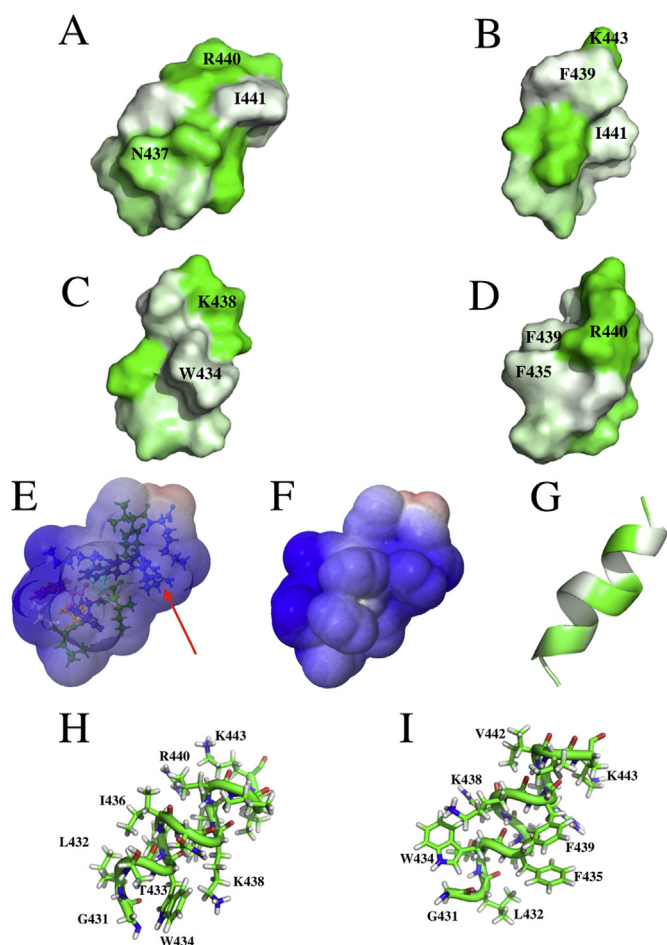
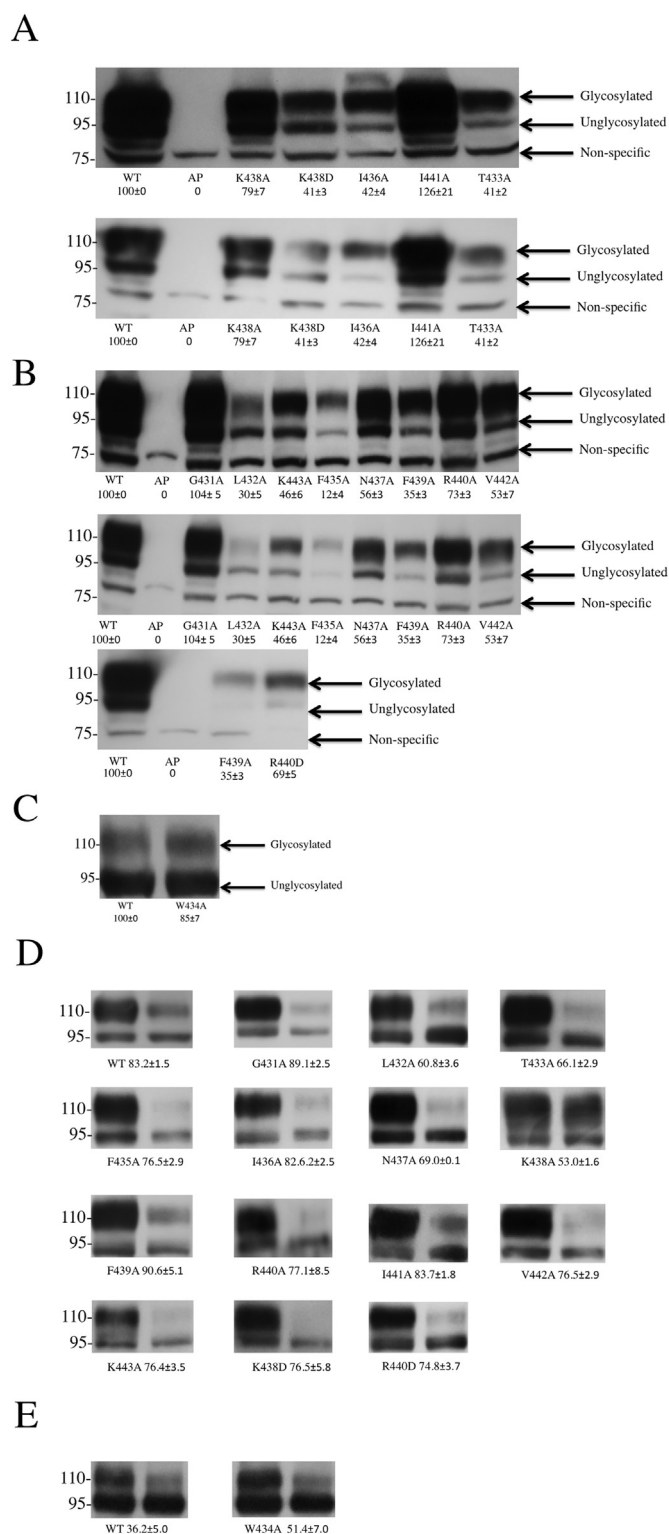


**Fig. 3.** Structural representations of IL5 peptide. A-D, Representative hydrophobic surface structure of IL5 peptide in different orientations created with PyMOL. Green indicates hydrophilic residues and white indicates hydrophobic residues. The intensity of the green or white colors indicates the degree of hydrophobicity or hydrophilicity of each amino acid residue respectively. A, Front view, B, Rotated 90°, C, Rotated 180°, D, Rotated 270°. For all figs. N-terminal in the bottom left corner and C-terminal in the top right. E, F Electrostatic potential map of IL5 peptide. Cationic regions are blue and anionic regions are red. N-terminal in the bottom left corner and C-terminal in the top right. Red arrow denotes Arg440. G, Ribbon diagram depicting the IL5 peptide. Hydrophobic side chains are drawn as sticks. H, Structural diagram depicting the IL5 peptide illustrating Lys-Trp-Ser-stick with Lys438 close to Trp434. I, Sticks-ribbon-ring lock diagram depicting the IL5 peptide.

WT protein.

To determine the level of NHE1 activity that is independent of protein expression level and surface targeting we corrected for surface processing and expression levels (Fig. 5B). It appeared to be that the activity level of mutants F435A, N437 N, K438A, I441A, V442A, K443A and R440D were comparable with the WT protein after correction. The mutants G431A, L432A, T433A and F439A had an activity level that is between 50% - 70% of the WT protein. Two mutants, I436A and R440A, had an activity level of 40% and 20% respectively. Lastly, the K438D protein had an activity level that was slightly greater than the WT protein after correction.

The experiments above were done with an ammonium chloride pulse resulting in a maximal, or near maximal activation of the NHE1 protein. To determine the activation of the Na<sup>+</sup>/H<sup>+</sup> exchanger over varying pH<sub>i</sub>, we calculated the buffering capacity of the wild type and several mutant cell lines and then determined the proton flux activity at varying pH<sub>i</sub>, as described in the Materials and methods. Fig. 4 (supplement) illustrates the buffering capacity of the wild type and mutant



(caption on next page)

cell lines I436A, R440A, R440D, G431A, T433A, N437A and K443A. There were small differences between the wild type and the mutants.

To examine the proton flux of NHE1 at varying pH<sub>i</sub>, cells containing wild type and mutant NHE1 were acidified to varying degrees as described in the “Materials and methods”. Proton flux was then examined using the buffering capacity of the particular cell type. The results are shown in Fig. 6. Wild type NHE1 had a V<sub>max</sub> of approximately 10 and was half maximally activated at a pH<sub>i</sub> of 6.2. All of the mutants had

**Fig. 4.** Analysis of wild type and mutant NHE1 protein expression and targeting. A–C, Western blot of whole cell lysates of stable cell lines expressing stably transfected (A, B) or transiently transfected IL5 mutants. A, K443A, K438D, I436A, I441A, T433A mutations are as indicated (Upper panel longer film exposure, lower panel shorter film exposure). B, G431A, L432A, K443A, F435A, N437A, F439A, R440A, V442A, (Upper panel longer film exposure, middle panel shorter film exposure). F439A, R440D lower panel. C, Western blot of whole cell lysates of transiently transfected cells expressing wild type and IL5 mutant W434A Na<sup>+</sup>/H<sup>+</sup> exchanger protein. A–C, 100 µg of total protein was loaded in each lane. Numbers below the lanes indicate the amount of NHE1 protein relative to wild type NHE. Mean values (n = 3) were obtained from densitometric scans of both the 110-kDa (upper) and 95-kDa (lower) bands. AP-1 cells refer to AP-1 cells mock transfected. D, E, Cell surface localization of wild type and IL5 mutant Na<sup>+</sup>/H<sup>+</sup> exchanger proteins expressed in AP-1. Equal amounts of total cell lysate (left lane) and unbound intracellular lysate (right lane) were examined by western blotting with anti-HA antibody. WT are cells stably expressing wild type NHE1. The percent of the total NHE1 protein found on the plasma membrane is indicated for each cell type and are mean ± S.E. n ≥ 4 determinations. Autoradiography exposure times were increased for mutants expressing lower levels of protein.

proton flux reduced including I436A, R440A, R440D, T433A, N437A and K437A (Fig. 6B–H). In some cases (I436A, R440A, R440D, G431A, T433A, N437A and K443A) the V<sub>max</sub> was greatly reduced. Some of the mutants (I436A, R440D, T433A, and K443A) were greatly reduced in activity across all pHi's and were not responsive to pHi. It was not possible to fit an estimate of affinity and V<sub>max</sub> for some mutants (I436A, R440D) and others had a poor fit (T433A, K443A) but are shown for illustrative purposes. The R440A mutant responded to pHi increasing in activity with acidic pHi, reaching half of V<sub>max</sub> at pHi 6.5. Activity was greatly reduced to about 1/5 the level of the wild type NHE1 protein. There was a similar effect on the G431A mutant that was also decreased in maximal activity. For both R440A and G431A, changes in the level of expression and targeting, could not account for effects on maximal activity.

#### 4. Discussion

In this study we examined the structure and function of IL5 of the mammalian Na<sup>+</sup>/H<sup>+</sup> exchanger isoform one. The regulation of activity of this protein is of great interest for both physiology and pathology. Stimulation of NHE1 activity promotes cell growth, proliferation, motility and differentiation [2, 3]. NHE1 is also a trigger for several pathologies. Elevated NHE1 activity promotes breast cancer cell invasion and metastasis [4–7]. Elevated NHE1 activity is also involved in heart disease. The increased activity triggers damage that occurs during myocardial ischemia and reperfusion and also promotes heart hypertrophy [8–11]. Thus the study of the mechanism of regulation of activity of the protein is of significant interest.

##### 4.1. Critical residues of IL5

Examination of the residues critical in NHE1 function revealed that many residues of the IL5 loop are sensitive to mutation and critical to activity of the protein. When compared with unaltered NHE1 protein, we found that mutation to alanine resulted in 11 mutant proteins (i.e. G431A, L432A, T433A, F435A I436A, N437A, K438A, F439A, R440A, V442A, K443A) in which the activity was significantly reduced. The IL5 loop is therefore very sensitive to alteration in many of the side chains of the amino acids. The cause of the defects in activity could either be due to defective expression and targeting. or a direct effect of the mutation that alters the intrinsic activity or pH responsiveness of the protein. The mutants: G431A, L432A, T433A, F435A, I436A, N437A, K438A, F439A, R440A, V442A, K443A, K438D, and R440D were assayed for activity with a large, acid load induced with ammonium chloride. Correction for the amount of protein or targeting of the

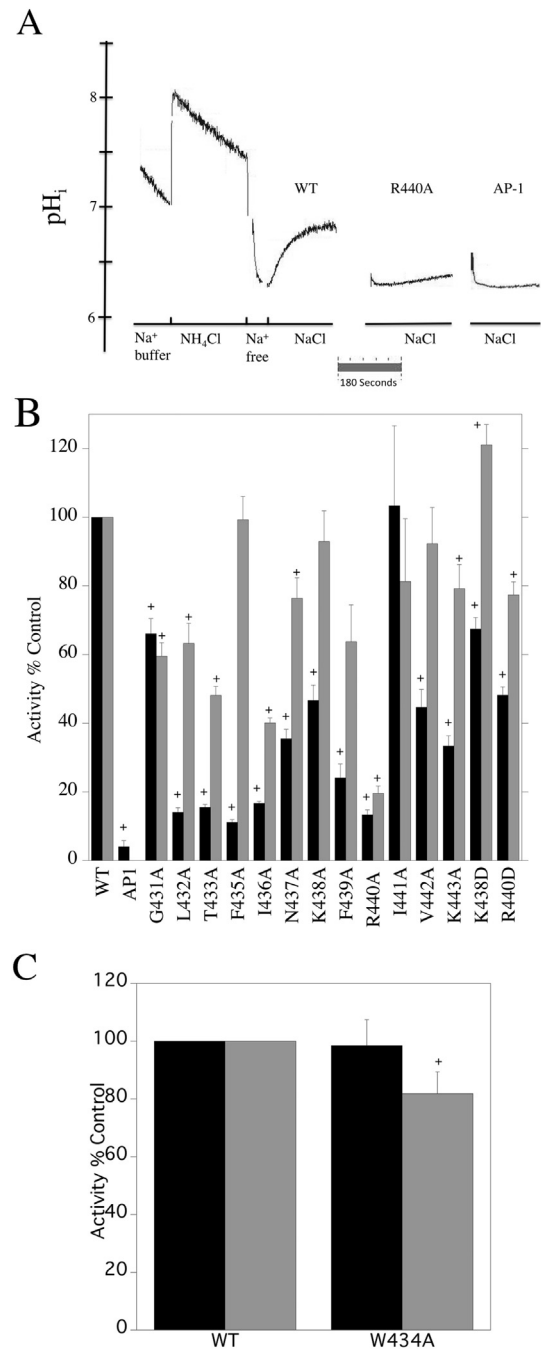


**Fig. 5.** Na<sup>+</sup>/H<sup>+</sup> exchanger protein activity was assayed in stably transfected AP-1 cells. Cells were in Na<sup>+</sup> buffer for three minutes. Then were treated with NH<sub>4</sub>Cl for three minutes, after the NH<sub>4</sub>Cl treatment, there was a brief Na<sup>+</sup> containing free treatment to induce acidosis. This was followed by a treatment in Na<sup>+</sup> containing buffer to induce NHE1 activity. A three-point pH calibration at pH 8, 7, and 6 was performed after every assay. A, example of Na<sup>+</sup>/H<sup>+</sup> exchanger activity assay for WT NHE1 (positive control) and recovery phases for R440A and AP-1 cells. B, C, Summary of rate of recovery of AP-1 cells after an acute acid load for stably transfected (B) and transiently transfected (C) cells. The mean activity of WT stably transfected with NHE1 was 0.021 ΔpH/min, and this value was set to 100% and other activities are a percent of those of WT. Values are the mean ± 8–10 determinations. Results are shown for mean activity of both uncorrected (black) and normalized for levels of surface processing and expression levels (gray). + indicates IL5 mutant activities that are significantly lower than that of WT NHE1 at P < 0.05.

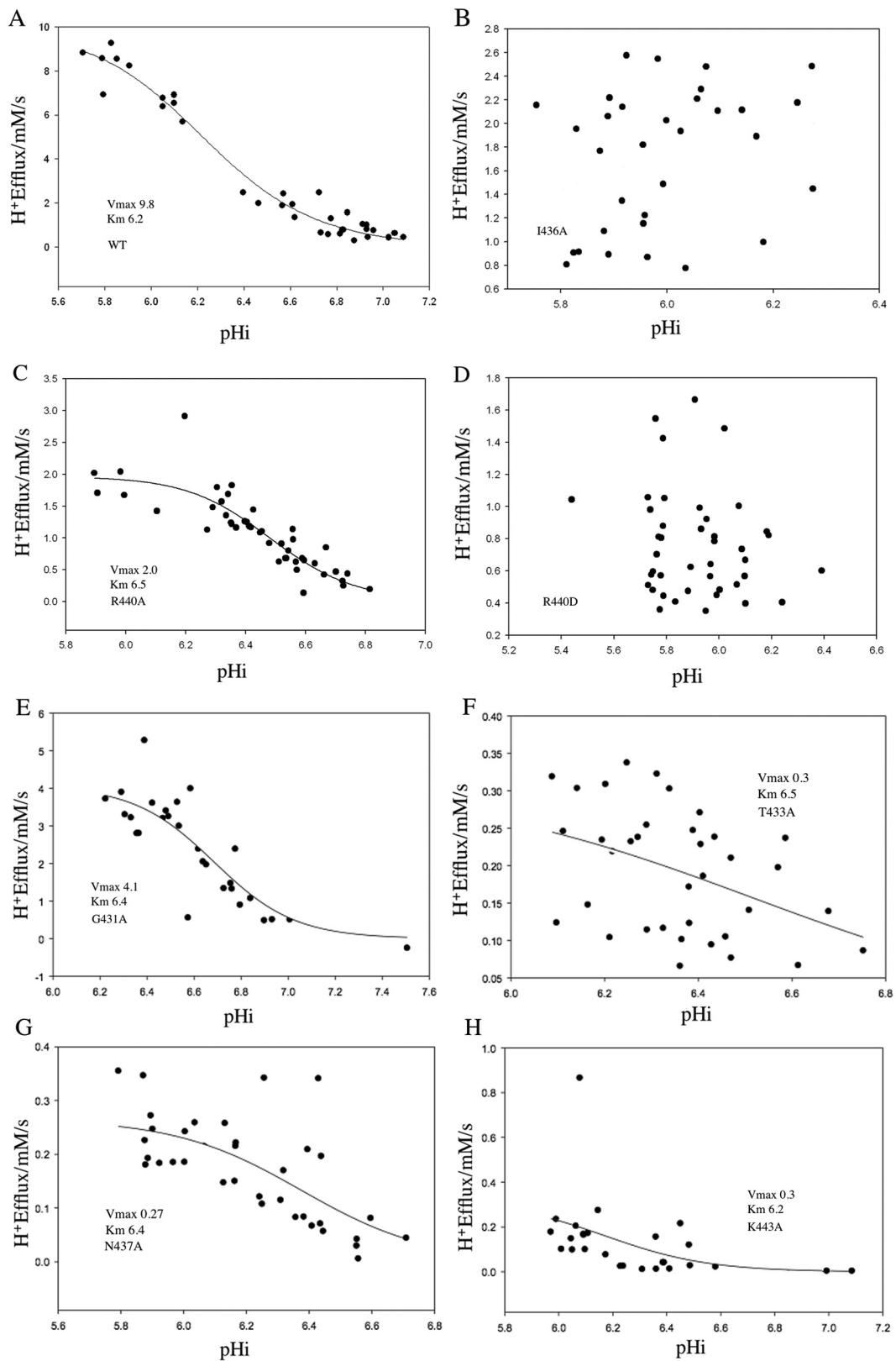


**Fig. 6.** Dependence of proton efflux on intracellular pH in wild type and mutant cell lines. Cells were incubated with varying concentrations of ammonium chloride that was removed to induce different degrees of acid load. Recovery was determined in  $Na^+$ -containing (135 mM) buffer. Proton efflux was calculated from the initial rate of recovery and the buffering capacity as described in the [Materials and methods](#). WT, wild type, mutants were I436A, R440A, R440D, G431A, T433A, N437A and K443A.

protein showed that under these conditions the protein was partially functional (Fig. 5). In the mutant W434A correction for protein levels or targeting did not result in an activity comparable to controls, indicating that the mutation caused a defective NHE1 protein. Of the stable transfected mutant proteins, several mutants had defective activity partially caused by targeting or surface processing of the protein and partially affecting intrinsic activity of the protein directly. This included eight mutants of 7 amino acids, G431A, L432A, T433A, I436A, N437A, F439A, R440A, and R440D. This strongly suggests that many of the side chains of the amino acids in IL5 are critical in the function (and possibly in tertiary structure) of these proteins.

A more detailed examination of the kinetics of activity of the mutants I436A, R440A, R440D, G431A, T433A, N437A and K443A over varying intracellular pH (Fig. 6) revealed that proton flux and “pH sensing”, the responsiveness to  $\text{pH}_i$ , was severely compromised in all these mutants. The G431A mutant was the most active with the conservative mutation of Gly to Ala. Even this protein was only approximately half as active as wild type, despite having normal surface processing and expression levels. In contrast to wild type NHE1, the activity of many of these proteins was not responsive to changes in  $\text{pH}_i$ . Exceptions to this observation are mutants R440A and G431A, who were responsive to changes in  $\text{pH}_i$ . However, maximal velocity was reduced in both cases and this could not be accounted for by changes in protein expression or targeting.

We also made two other point mutations; K438D and R440D. These were independently mutated to aspartic acid to reverse the charge of these two amino acids. We found a significant decrease in activity in the K438D mutant. This reduction was due to reduced expression levels and surface targeting. A previous study [40] made a K438E mutation and reported no changes in activity, though details of expression and targeting were not provided. K438 is quite conserved (Fig. 1C) though in some species it is substituted for by another basic residue, Arg.

As noted above, the activity of the R440D mutant was reduced. Previous work [41, 42], examined the effect of R440D mutation on pH dependence of exchanger activity. They demonstrated that this mutation caused an acidic shift in the pH dependence of activity. It was suggested [41] that the R440D mutation modulates the affinity of the internal modifier site for protons. Mutations to Cys, His, Asp, Glu and Leu also caused acidic shifts as did mutation to Lys [42]. In our hands, the R440D mutation caused a decrease in activity of NHE1 when measured at strongly acidic  $\text{pH}_i$ . Additionally, activity over a wide pH range was impaired and this mutant was only weakly responsive to changes in intracellular pH. As noted above, we found that a R440A mutation had a significant effect with reduced activity. This indicated that a negative charge was not necessary for inhibition of activity though it was clear that mutation to Ala only had less of an effect than mutation to Asp. Taken together with the previous studies, [41, 42] it is clear that R440 is sensitive to mutation, and that mutations to this site cause defects in activity. Our results with mutation to Ala, suggest that even what is normally considered a benign mutation, has a significant effect, and that a change to an acidic residue is not required for inhibition of NHE1 activity. It may be that a precise steric bulkiness of the side chain is important for the structure of the protein, and/or the hydrophobic nature may result in differential binding or final positioning of the peptide. It is interesting that R440 is in the same face of the peptide as I436 (Fig. 3G). Both these amino acids showed the lowest activity after correction for expression levels and targeting. It may be that they form some kind of interface between IL5 and the regulatory tail, however further experiments are necessary to examine this hypothesis. R440 is very conserved across a number of species (Fig. 1C).

#### 4.2. Analysis of IL5 structure and function

High-resolution NMR analysis of the IL5 peptide indicated that the observed structure, or lack of, depended on the solvent. Initially we tried to determine the structure of IL5 peptide when dissolved in DMSO.

DMSO has an intermediate dielectric constant of approximately  $\sim 46$  [43] and is therefore similar to a membrane interface [44]. It was hoped that DMSO would result in a reasonable mimetic of the environment experienced by the peptide loop. In previous studies, Katragadda et al. [37] showed that NMR structures of isolated loops from bacteriorhodopsin in DMSO adopted structures equivalent to the known crystal structure of the protein. In addition, we previously examined two extracellular loops (EL2 and EL4) of NHE1 elucidated in a DMSO environment [17, 36]. In our previous findings [17], EL2 had inter-helical loops in aqueous or DMSO solvents. For EL4, possibly due to the short length of the peptide, the loop was unstructured and flexible [36]. In DMSO however, IL5 appeared to be completely random coil as indicated by the poorly resolved NH resonances in the peptide, and the lack of NOE cross-peaks. A temperature titration was performed for the peptide when dissolved in DMSO (Fig. 2A). The 1D spectrum of the peptide in DMSO at 18 °C had the best resolution.

To obtain a defined secondary and tertiary structure, IL5 was dissolved in SDS. SDS micelles are a commonly used mimetic for determination of structure of peptides associated with biomembranes [45]. In the presence of SDS, there were no signs of precipitation. The initial spectra did show appropriate broadening as expected when moving from a free peptide in solution to a SDS micelle/membrane associated environment. Our first experiments involved a series of temperature titrations (Fig. 2B), and after evaluation of the spectra, 27 °C was chosen for the acquisition of all 2D spectra. This temperature gave the best resolution and most consistent line width providing the greatest confidence that we had a stable predominant structure for the peptide. Structures were then generated using CYANA 2.1 (Table 1). The assigned chemical shifts were determined as described above, and the carefully cleaned NOE peak list was given to CYANA to iteratively select the non-ambiguous versus ambiguously weighted cross-peaks. Restraints were determined by CYANA based on confidence and peak intensities. The final structure (Fig. 3) indicated that IL5 peptide is highly alpha helical. Another interesting observation is that K438 is very close to W434.

Overall, our study shows that IL5 is a region of NHE1 that is critical in activity, targeting, expression and is influential on pH sensing of the  $\text{Na}^+/\text{H}^+$  exchanger, isoform 1. Our results show that surprisingly, many amino acids of IL5 are critical for function affecting activity directly and/or affecting targeting and expression. Virtually the entire intracellular loop is an essential part of the NHE1 protein with a propensity towards a structure that may be important in function.

#### Transparency document

The Transparency document associated this article can be found, in online version.

#### Acknowledgements

Supported by funding to LF by CIHR (MOP-97816).

#### Appendix A. Supplementary data

Supplementary data to this article can be found online at <https://doi.org/10.1016/j.bbamem.2018.07.014>.

#### References

- [1] L. Fliegel, Molecular biology of the myocardial  $\text{Na}^+/\text{H}^+$  exchanger, *J. Mol. Cell. Cardiol.* 44 (2008) 228–237.
- [2] S. Grinstein, D. Rotin, M.J. Mason,  $\text{Na}^+/\text{H}^+$  exchange and growth factor-induced cytosolic pH changes. Role in cellular proliferation, *Biochim. Biophys. Acta* 988 (1989) 73–97.
- [3] L. Shrode, A. Cabado, G. Goss, S. Grinstein, Role of the  $\text{Na}^+/\text{H}^+$  antiporter isoforms in cell volume regulation, in: L. Fliegel (Ed.), *The  $\text{Na}^+/\text{H}^+$  Exchanger*, R.G. Landes Company, 1996, pp. 101–122.

- [4] G. Busco, R.A. Cardone, M.R. Greco, A. Bellizzi, M. Colella, E. Antelmi, M.T. Mancini, M.E. Dell'Aquila, V. Casavola, A. Paradiso, S.J. Reshkin, NHE1 promotes invadopodial ECM proteolysis through acidification of the peri-invadopodial space, *FASEB J.* 24 (2010) 3903–3915.
- [5] C. Stock, R.A. Cardone, G. Busco, H. Krahlhng, A. Schwab, S.J. Reshkin, Protons extruded by NHE1: digestive or glue? *Eur. J. Cell Biol.* 87 (2008) 591–599.
- [6] S. Harguindey, G. Orive, J. Luis Pedraz, A. Paradiso, S.J. Reshkin, The role of pH dynamics and the Na<sup>+</sup>/H<sup>+</sup> antiporter in the etiopathogenesis and treatment of cancer. Two faces of the same coin—one single nature, *Biochim. Biophys. Acta* 1756 (2005) 1–24.
- [7] A. Paradiso, R.A. Cardone, A. Bellizzi, A. Bagorda, L. Guerra, M. Tommasino, V. Casavola, S.J. Reshkin, The Na<sup>+</sup>-H<sup>+</sup> exchanger-1 induces cytoskeletal changes involving reciprocal RhoA and Rac1 signaling, resulting in motility and invasion in MDA-MB-435 cells, *Breast Cancer Res.* 6 (2004) R616–R628.
- [8] M. Karmazyn, Q. Liu, X.T. Gan, B.J. Brix, L. Fliegel, Aldosterone increases NHE-1 expression and induces NHE-1-dependent hypertrophy in neonatal rat ventricular myocytes, *Hypertension* 42 (2003) 1171–1176.
- [9] L. Fliegel, Regulation of myocardial Na<sup>+</sup>/H<sup>+</sup> exchanger activity, *Basic Res. Cardiol.* 96 (2001) 301–305.
- [10] R.M. Mentzer Jr., R.D. Lasley, A. Jessel, M. Karmazyn, Intracellular sodium hydrogen exchange inhibition and clinical myocardial protection, *Ann. Thorac. Surg.* 75 (2003) S700–S708.
- [11] H.J. Lang, Chemistry of NHE inhibitors, in: M. Karmazyn, M. Avkiran, L. Fliegel (Eds.), *The Na<sup>+</sup>/H<sup>+</sup> Exchanger, From Molecular to Its Role in Disease*, Kluwer academic Publishers, Boston/Dordrecht/London, 2003, pp. 239–253 (318p).
- [12] E. Murphy, D.G. Allen, Why did the NHE inhibitor clinical trials fail? *J. Mol. Cell. Cardiol.* 46 (2009) 137–141.
- [13] V. Munoz, F.J. Blanco, L. Serrano, The hydrophobic-staple motif and a role for loop-residues in alpha-helix stability and protein folding, *Nat. Struct. Biol.* 2 (1995) 380–385.
- [14] M.M. Zhao, R.J. Gaivin, D.M. Perez, The third extracellular loop of the beta2-adrenergic receptor can modulate receptor/G protein affinity, *Mol. Pharmacol.* 53 (1998) 524–529.
- [15] E.R. Slepko, J.K. Rainey, B.D. Sykes, L. Fliegel, Structural and functional analysis of the Na(+)/H(+) exchanger, *Biochem. J.* 401 (2007) 623–633.
- [16] R. Murtazina, B.J. Booth, B.L. Bullis, D.N. Singh, L. Fliegel, Functional analysis of polar amino-acid residues in membrane associated regions of the NHE1 isoform of the mammalian Na<sup>+</sup>/H<sup>+</sup> exchanger, *Eur. J. Biochem.* 268 (2001) 4674–4685.
- [17] B.L. Lee, X. Li, Y. Liu, B.D. Sykes, L. Fliegel, Structural and functional analysis of extracellular loop 2 of the Na(+)/H(+) exchanger, *Biochim. Biophys. Acta* 1788 (2009) 2481–2488.
- [18] A. Khadilkar, P. Iannuzzi, J. Orlowski, Identification of sites in the second exo-membrane loop and ninth transmembrane helix of the mammalian Na<sup>+</sup>/H<sup>+</sup> exchanger important for drug recognition and cation translocation, *J. Biol. Chem.* 276 (2001) 43792–43800.
- [19] S. Wakabayashi, T. Pang, X. Su, M. Shigekawa, A novel topology model of the human Na<sup>+</sup>/H<sup>+</sup> exchanger isoform 1, *J. Biol. Chem.* 275 (2000) 7942–7949.
- [20] M. Landau, K. Herz, E. Padan, N. Ben-Tal, Model structure of the Na<sup>+</sup>/H<sup>+</sup> exchanger 1 (NHE1): functional and clinical implications, *J. Biol. Chem.* 282 (2007) 37854–37863.
- [21] Y. Liu, A. Basu, X. Li, L. Fliegel, Topological analysis of the Na/H exchanger, *Biochim. Biophys. Acta* 1848 (2015) 2385–2393.
- [22] T. Hisamitsu, K. Yamada, T.Y. Nakamura, S. Wakabayashi, Functional importance of charged residues within the putative intracellular loops in pH regulation by Na<sup>+</sup>/H<sup>+</sup> exchanger NHE1, *FEBS J.* 274 (2007) 4326–4335.
- [23] P. Guntert, C. Mumenthaler, K. Wuthrich, Torsion angle dynamics for NMR structure calculation with the new program DYANA, *J. Mol. Biol.* 273 (1997) 283–298.
- [24] K. Wuthrich, *NMR of Proteins and Nucleic Acids*, Wiley, New York, 1986.
- [25] F. Delaglio, S. Grzesiek, G.W. Vuister, G. Zhu, J. Pfeifer, A. Bax, NMRPipe: a multidimensional spectral processing system based on UNIX pipes, *J. Biomol. NMR* 6 (1995) 277–293.
- [26] B.A. Johnson, R.A. Blevins, NMRView: a computer program for the visualization and analysis of NMR data, *J. Biomol. NMR* 4 (1994) 603–614.
- [27] B.A. Johnson, R.A. Blevins, NMRView: a computer program for the visualization and analysis of NMR data, *J. Biomol. NMR* 4 (1994) 603–614.
- [28] E.R. Slepko, J.K. Rainey, X. Li, Y. Liu, F.J. Cheng, D.A. Lindhout, B.D. Sykes, L. Fliegel, Structural and functional characterization of transmembrane segment IV of the NHE1 isoform of the Na<sup>+</sup>/H<sup>+</sup> exchanger, *J. Biol. Chem.* 280 (2005) 17863–17872.
- [29] E. Slepko, J. Ding, J. Han, L. Fliegel, Mutational analysis of potential pore-lining amino acids in TM IV of the Na(+)/H(+) exchanger, *Biochim. Biophys. Acta* 1768 (2007) 2882–2889.
- [30] J. Ding, J.K. Rainey, C. Xu, B.D. Sykes, L. Fliegel, Structural and functional characterization of transmembrane segment VII of the Na<sup>+</sup>/H<sup>+</sup> exchanger isoform 1, *J. Biol. Chem.* 281 (2006) 29817–29829.
- [31] N.L. Silva, H. Wang, C.V. Harris, D. Singh, L. Fliegel, Characterization of the Na<sup>+</sup>/H<sup>+</sup> exchanger in human choriocarcinoma (BeWo) cells, *Pflugers Arch. - Eur. J. Physiol.* 433 (1997) 792–802.
- [32] A. Kumar, G. Wagner, R.R. Ernst, K. Wuthrich, Studies of J-connectives and selective 1H-1H Overhauser effects in H2O solutions of biological macromolecules by two-dimensional NMR experiments, *Biochem. Biophys. Res. Commun.* 96 (1980) 1156–1163.
- [33] D. Neuhaus, M.P. Williamson, The nuclear Overhauser effect in structural and conformation analysis, *Methods Stereochem. Anal.* xxvii (2000) 619.
- [34] R. Ordog, PyDeT, a PyMOL plug-in for visualizing geometric concepts around proteins, *Bioinformatics* 2 (2008) 346–347.
- [35] N.A. Baker, D. Sept, S. Joseph, M.J. Holst, J.A. McCammon, Electrostatics of nanosystems: application to microtubules and the ribosome, *Proc. Natl. Acad. Sci. U. S. A.* 98 (2001) 10037–10041.
- [36] B.L. Lee, Y. Liu, X. Li, B.D. Sykes, L. Fliegel, Structural and functional analysis of extracellular loop 4 of the Nhe1 isoform of the Na(+)/H(+) exchanger, *Biochim. Biophys. Acta* 1818 (2012) 2783–2790.
- [37] M. Katragadda, J.L. Alderfer, P.L. Yeagle, Solution structure of the loops of bacteriorhodopsin closely resembles the crystal structure, *Biochim. Biophys. Acta* 1466 (2000) 1–6.
- [38] K.G. Fleming, D.M. Engelman, Specificity in transmembrane helix-helix interactions can define a hierarchy of stability for sequence variants, *Proc. Natl. Acad. Sci. U. S. A.* 98 (2001) 14340–14344.
- [39] X. Li, Y. Liu, B.V. Alvarez, J.R. Casey, L. Fliegel, A novel carbonic anhydrase II binding site regulates NHE1 activity, *Biochemistry* 45 (2006) 2414–2424.
- [40] J. Lacroix, M. Poet, C. Maehrel, L. Counillon, A mechanism for the activation of the Na/H exchanger NHE-1 by cytoplasmic acidification and mitogens, *EMBO Rep.* 5 (2004) 91–96.
- [41] S. Wakabayashi, T. Hisamitsu, T. Pang, M. Shigekawa, Kinetic dissection of two distinct proton binding sites in Na<sup>+</sup>/H<sup>+</sup> exchangers by measurement of reverse mode reaction, *J. Biol. Chem.* 278 (2003) 43580–43585.
- [42] S. Wakabayashi, T. Hisamitsu, T. Pang, M. Shigekawa, Mutations of Arg440 and Gly455/Gly456 oppositely change pH sensing of Na<sup>+</sup>/H<sup>+</sup> exchanger 1, *J. Biol. Chem.* 278 (2003) 11828–11835.
- [43] W.M. Haynes, W.M. Haynes (Ed.), *CRC handbook of Chemistry and Physics*, 92nd ed., CRC Press, Boca Raton, FL, 2011.
- [44] N. Bordag, S. Keller, Alpha-helical transmembrane peptides: a "divide and conquer" approach to membrane proteins, *Chem. Phys. Lipids* 163 (2010) 1–26.
- [45] D.E. Warschawski, A.A. Arnold, M. Beauprand, A. Gravel, E. Chartrand, I. Marcotte, Choosing membrane mimetics for NMR structural studies of transmembrane proteins, *Biochim. Biophys. Acta* 1808 (2011) 1957–1974.

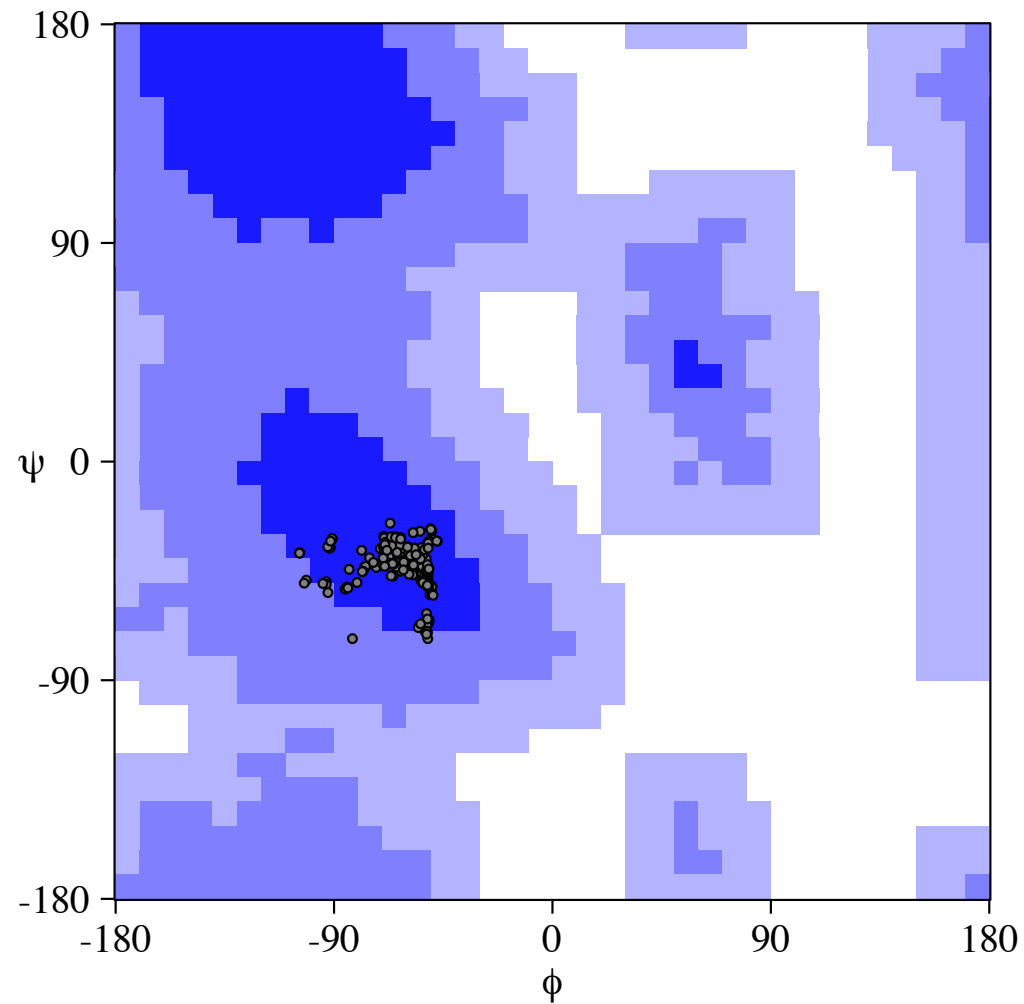


**Figure 1Supplement.** Ramachandran plot for IL5 protein showing steric hinderance. 95.9% in most favored region, 4.1% in additionally allowed regions, 0.0% in generously allowed regions and 0.0% in disallowed regions.

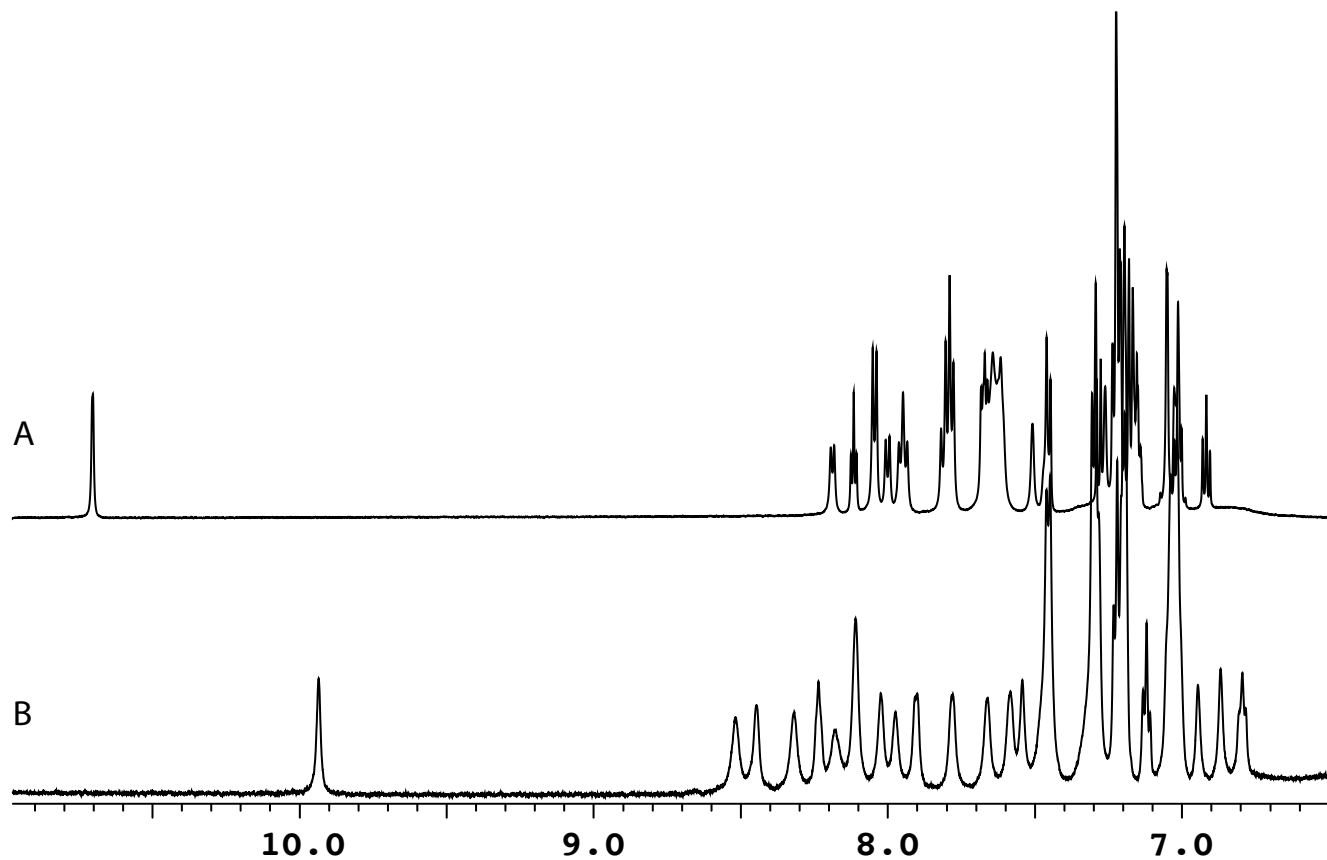


**Figure 2S** Comparison of 1D Spectra of IL5 in 2.8 mM of DMSO and 440 mM of SDS solution at their optimal temperatures. A. DMSO 18.1°C (top) B. SDS 27°C (bottom).

A

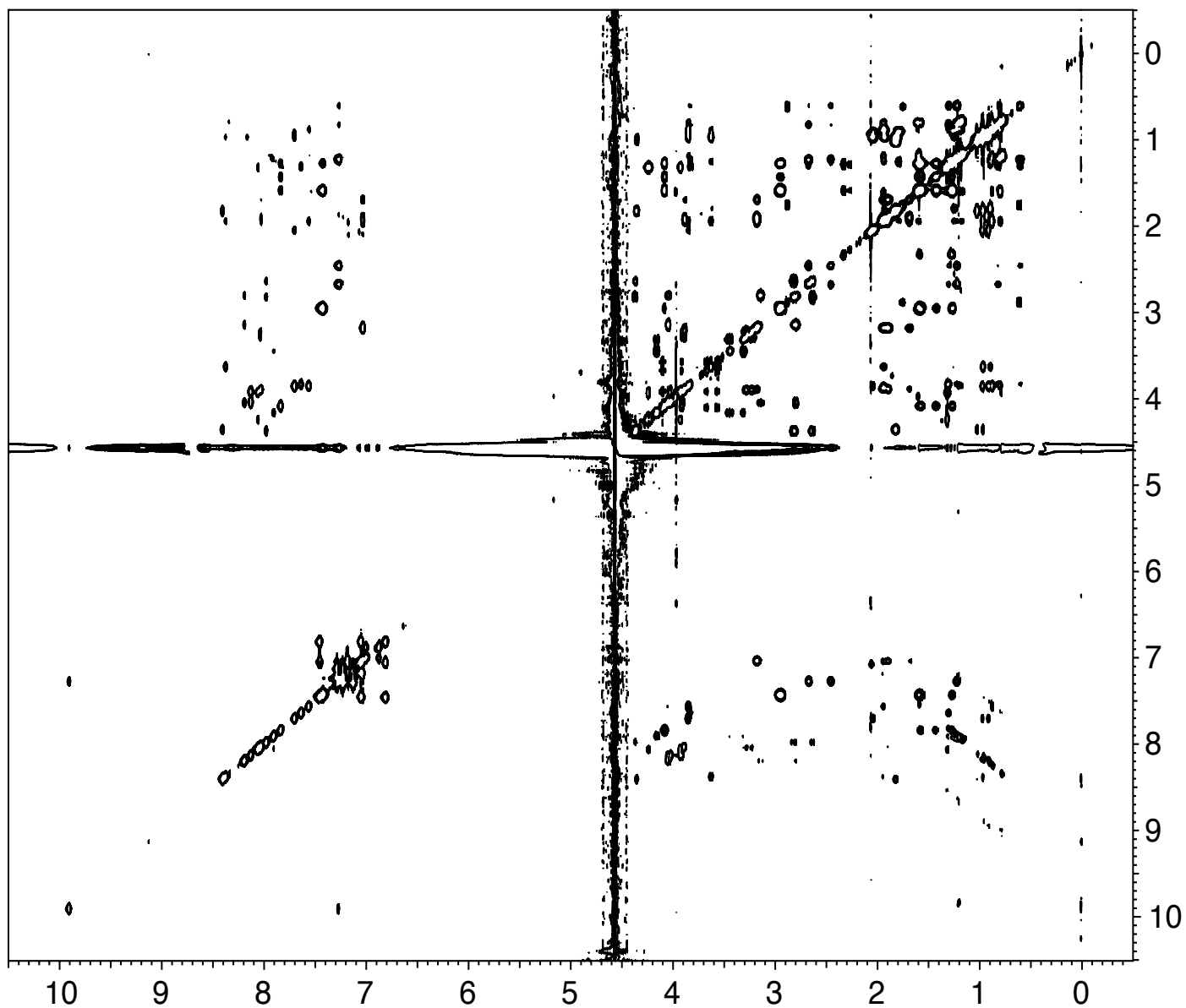


**Fig. 3ASupplement.** Spectra of IL5 in SDS solution. **A.** NOESY Spectrum of 5 mM IL5 peptide. The spectrum was recorded at 700 MHz with a mixing time of 150 ms at 40°C.

B

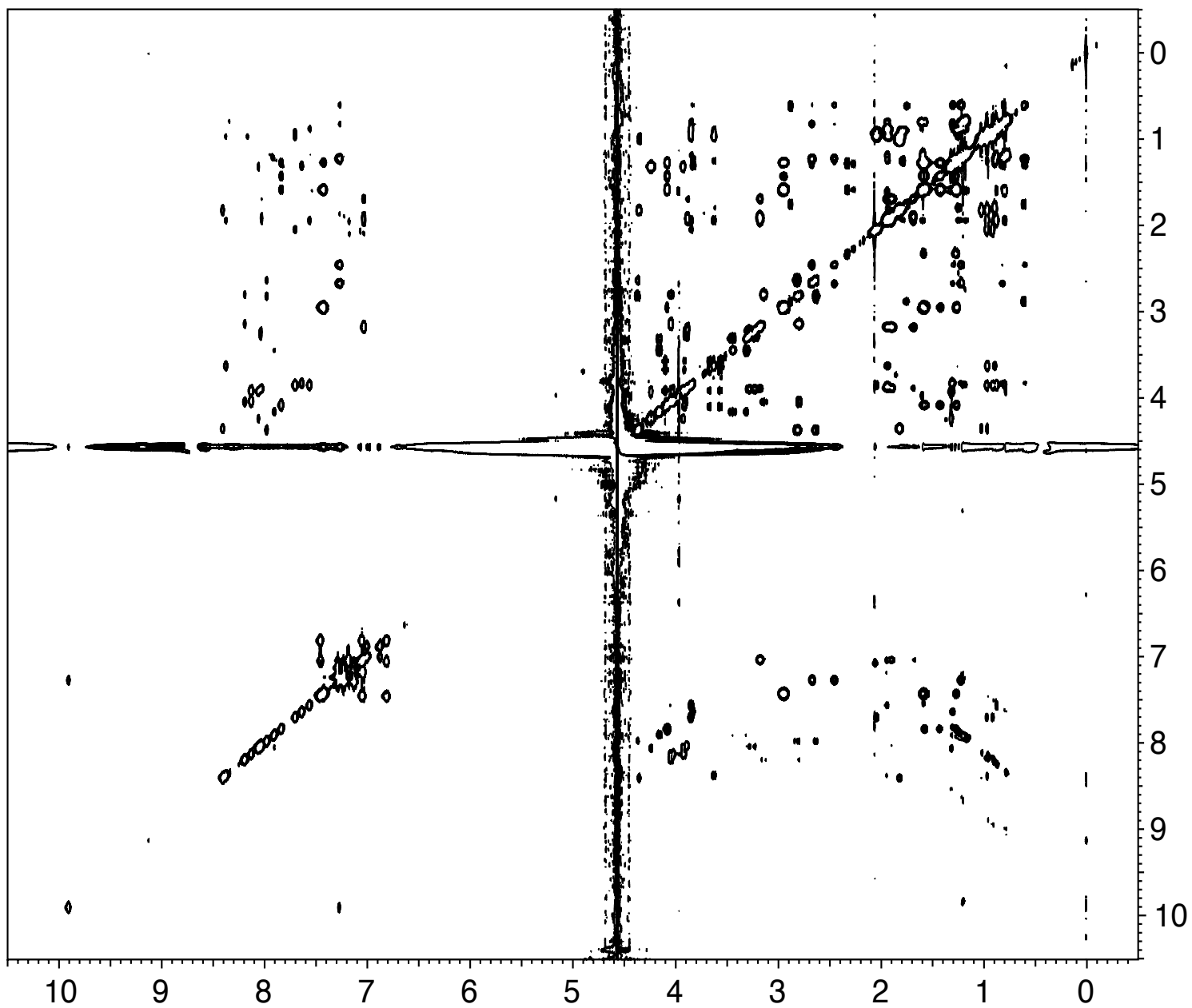


**Fig. 3BSupplement.** TOCSY Spectrum of 5 mM IL5 peptide. The spectrum was recorded at 700 MHz with a mixing time of 65 ms at 40°C.

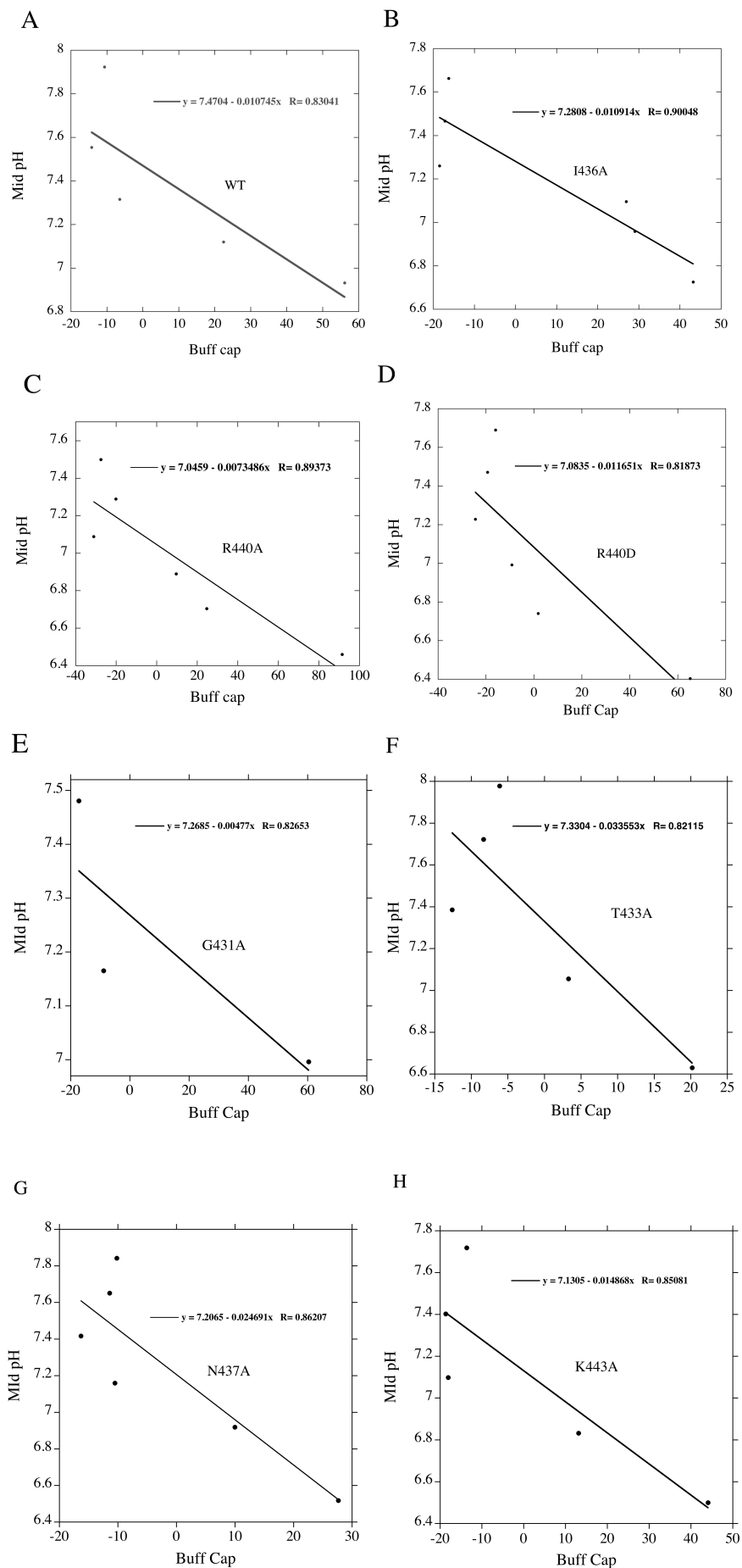


Fig. 4S. Buffering Capacity vs. Mid point pH. Buffering capacity was determined as described in the Materials and Methods. Wild type and mutant cell lines are shown.